

Supporting Information

Forming Layered Conjugated Porous BBL Structures

Sun-Hee Shin, Hyuk-Jun Noh, Young-Hyun Kim, Yoon-Kwang Im, Javeed Mahmood and Jong-Beom Baek**

School of Energy and Chemical Engineering, Center for Dimension-Controllable Organic Frameworks, Ulsan National Institute of Science and Technology (UNIST), 50 UNIST, Ulsan 44919, South Korea

* To whom correspondence should be addressed. E-mail: jbbaek@unist.ac.kr, javeed@unist.ac.kr Tel: +82-52-217-2510; Fax: +82-52-217-2639

KEYWORDS: Poly(benzoimidazobenzophenanthroline, BBL), ladder structure, fused organic network, high Q_{st} gas adsorption

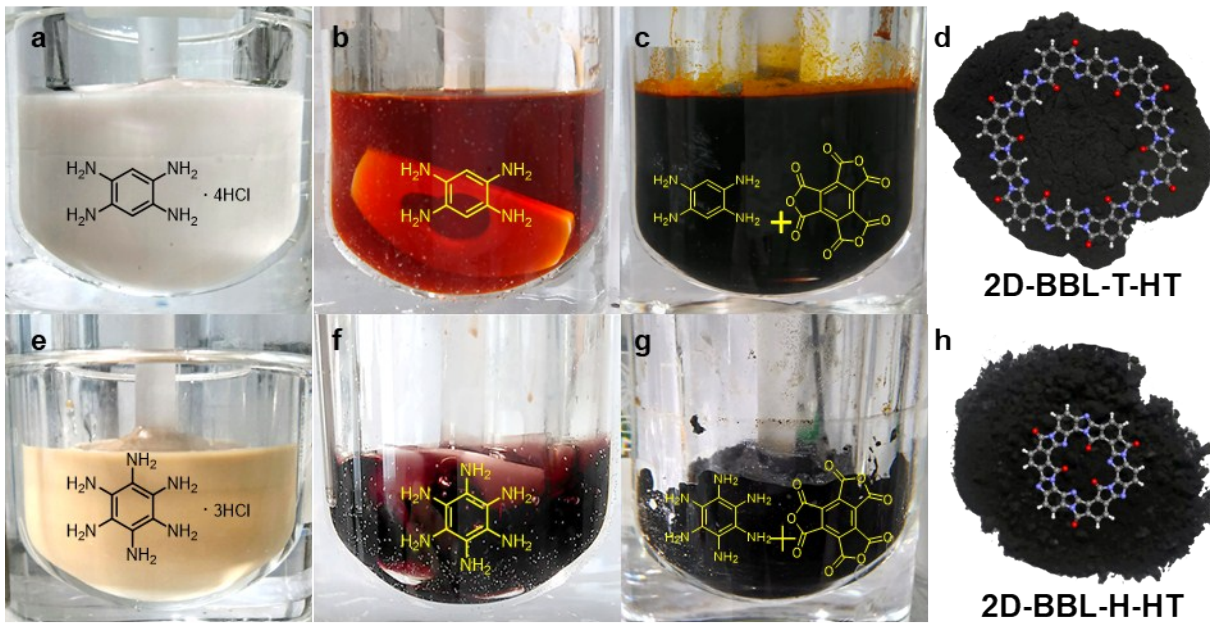


Fig. S1. Photographs taken during the synthesis of 2D-BBL-T and 2D-BBL-H; (a) Tetraaminobenzene (TAB) tertahydrochloride in PPA at room temperature, (b) after complete dehydrochlorination, the color of media changed from white to orange and transparent. (c) Polymerization with mellitic trianhydride (MTA) at 175 °C. (d) Photograph of as-synthesized 2D-BBL-T-HT. (e) Hexaaminobenzene (HAB) trihydrochloride in PPA at room temperature, (f) after complete dehydrochlorination, the color of media changed from light brown to red and transparent. (g) Polymerization with mellitic trianhydride (MTA) at 175 °C. (h) Photograph of as-synthesized 2D-BBL-H-HT.

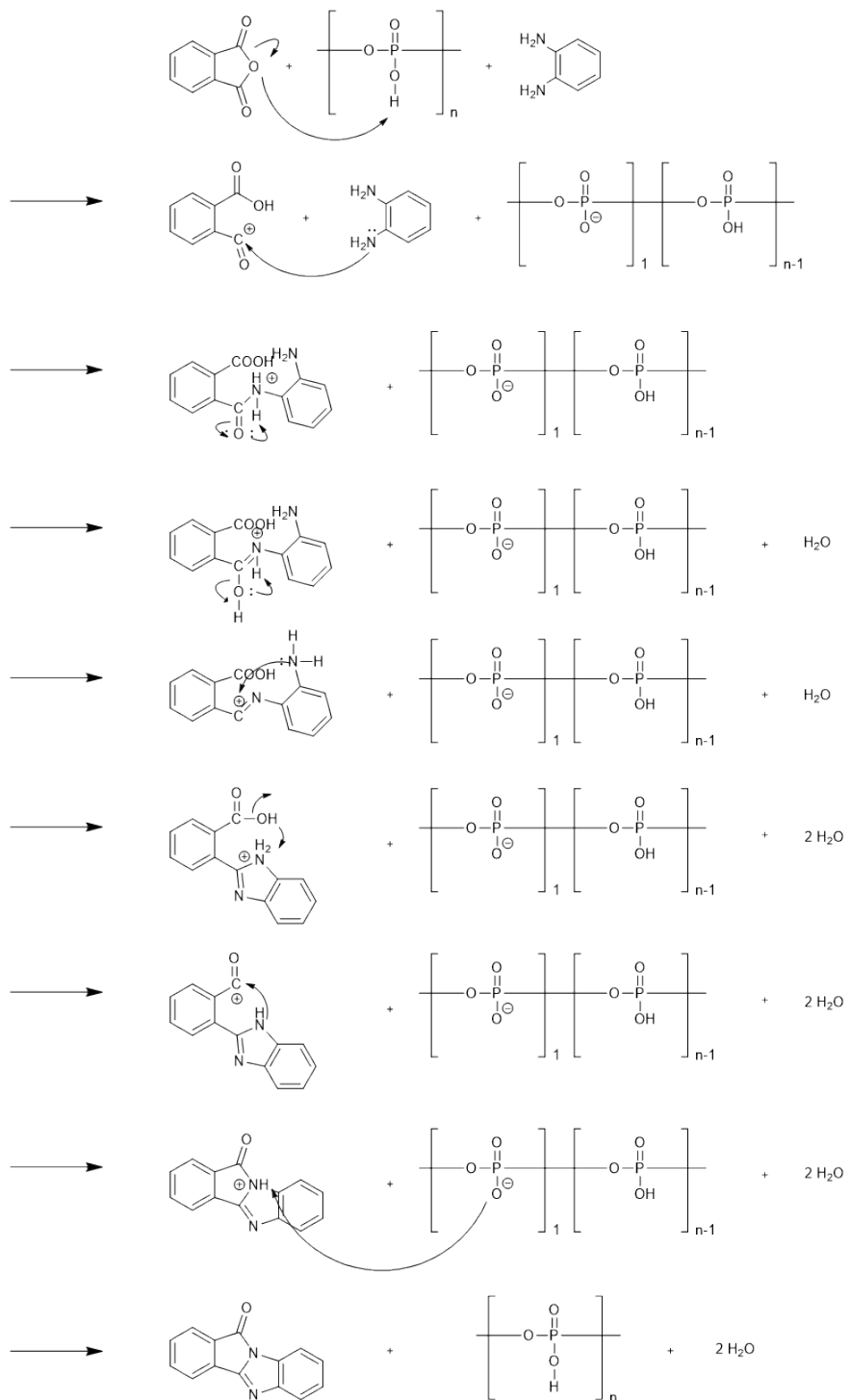


Fig. S2. The condensation mechanism for the formation of benzimidazobenzophenanthroline compounds in polyphosphoric acid (PPA), which plays as acid catalyst for dehydration and polar solvent for polymer.

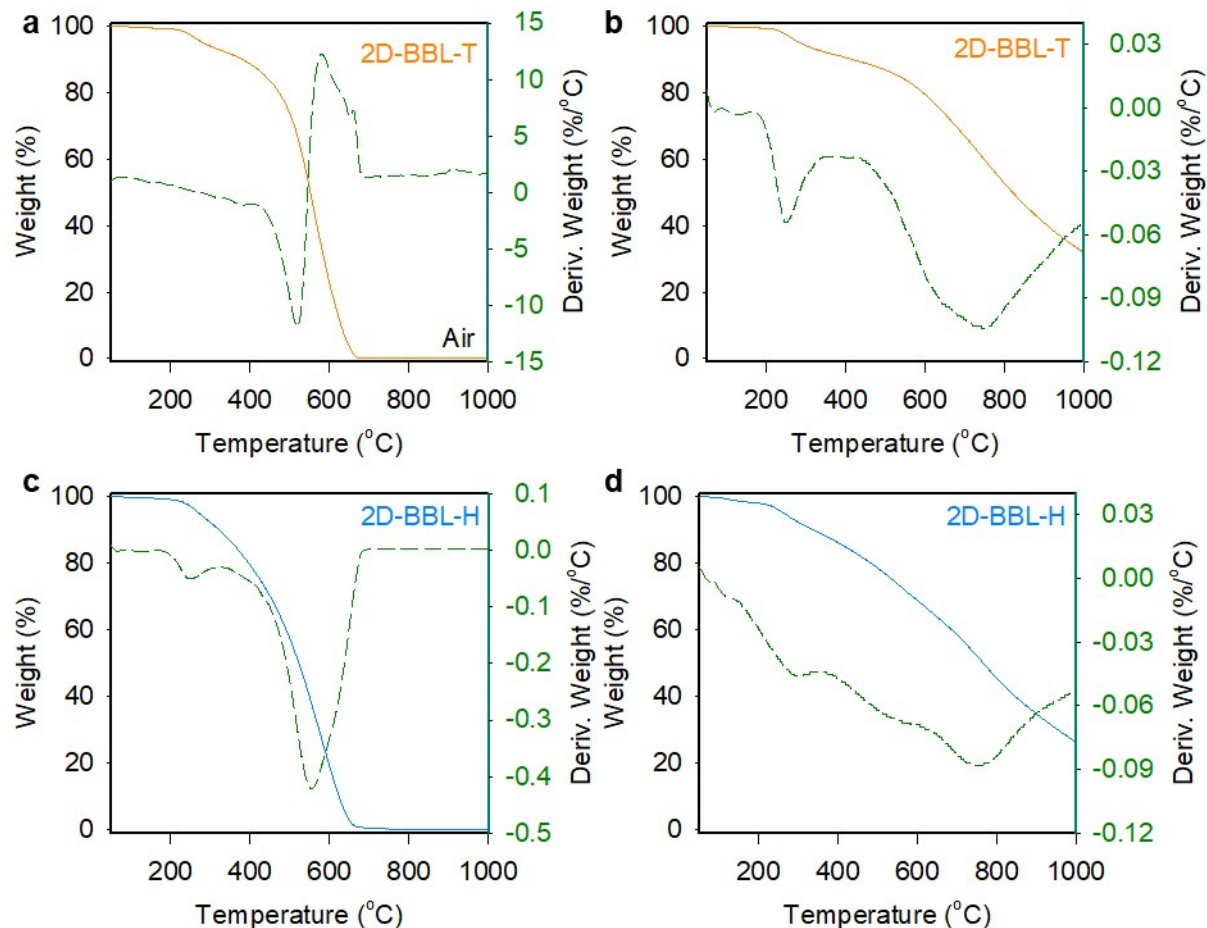


Fig. S3. TGA thermograms of 2D-BBL-T and 2D-BBL-H obtained with the ramping rate of $10\text{ }^{\circ}\text{C min}^{-1}$: (a, c) in air, (b, d) in nitrogen. In both air and nitrogen atmosphere, Heat-treated samples, 2D-BBL-T-HT and 2D-BBL-H-HT (**Figure 1a, b**) displayed significantly improved thermal stability, due to the removal of periphery amine ($-\text{NH}_2$) and carboxylic acid ($-\text{COOH}$) groups.

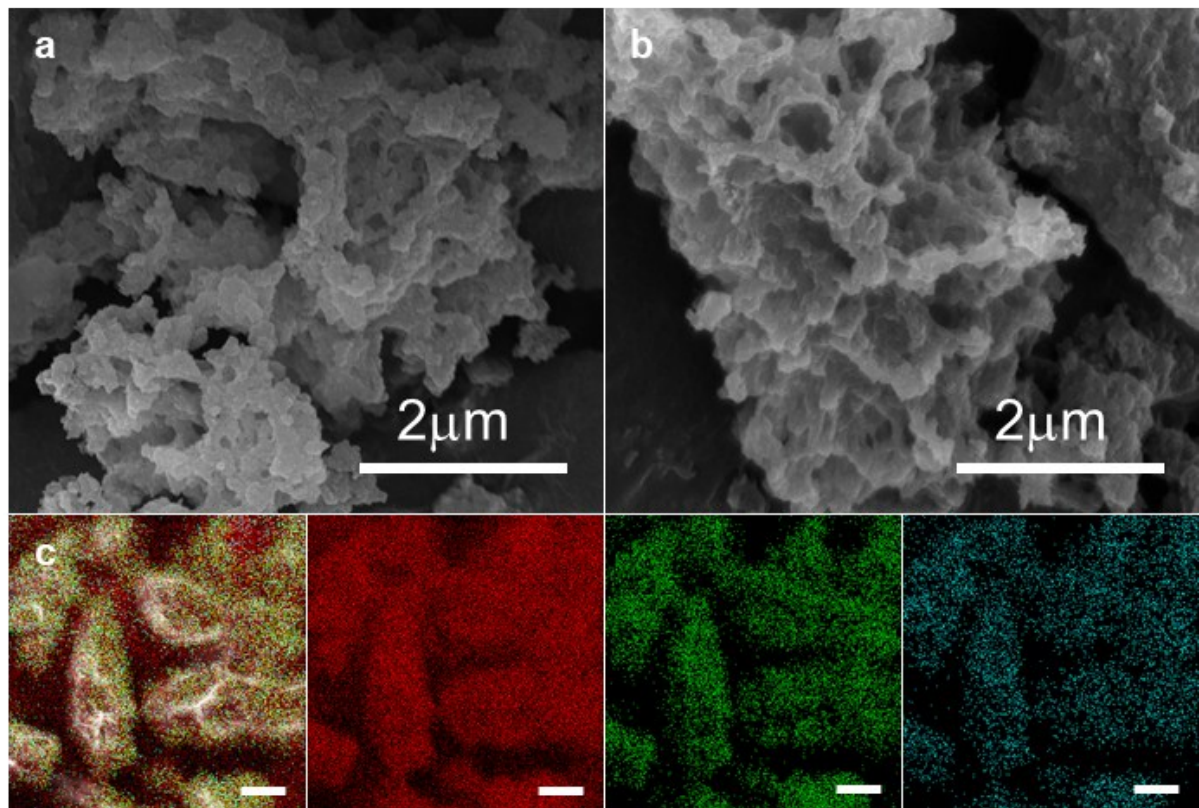


Fig. S4. SEM images: (a) 2D-BBL-T, (b) 2D-BBL-T-HT, (c) SEM image of 2D-BBL-T-HT with element mappings for all elements (red, green and cyan), carbon (red), nitrogen (green) and oxygen (cyan) in that order. Scale bars are 2 μ m.

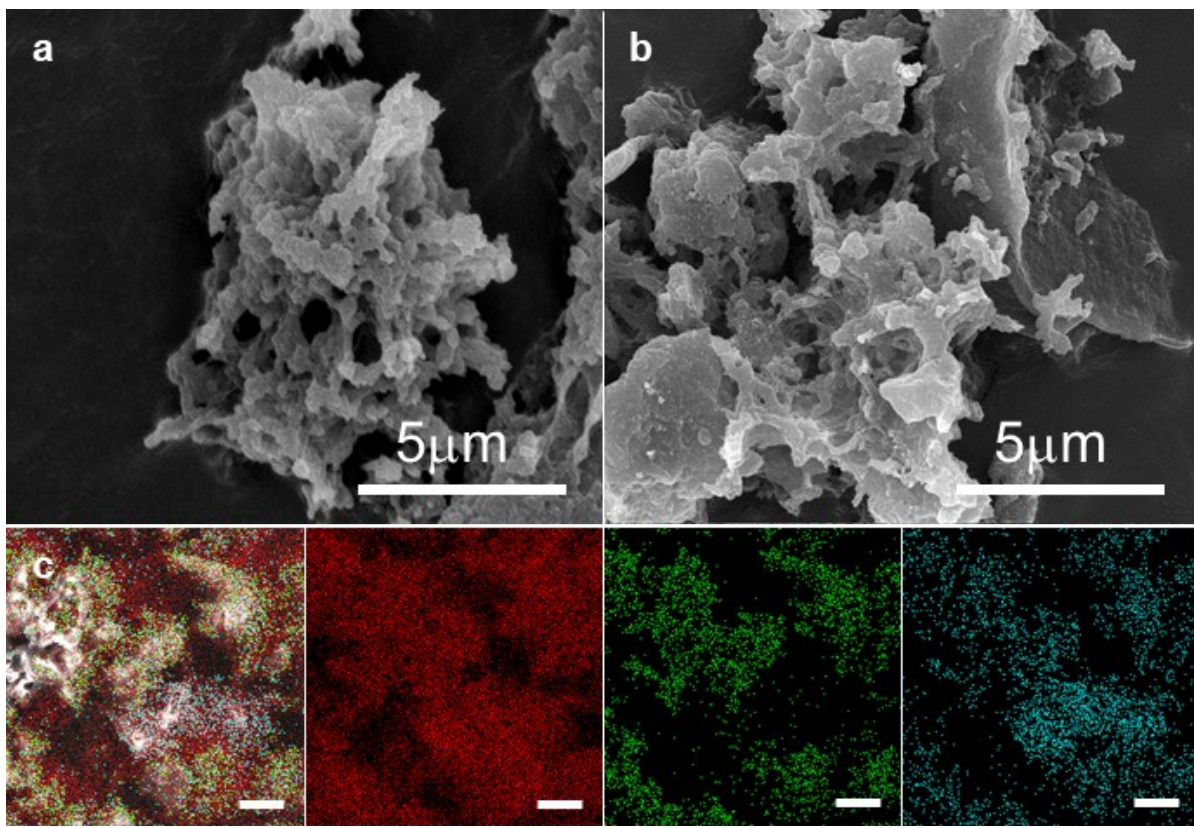


Fig. S5. SEM images: (a) 2D-BBL-H, (b) 2D-BBL-H-HT, (c) SEM image of 2D-BBL-H-HT with element mappings for all elements (red, green and cyan), carbon (red), nitrogen (green) and oxygen (cyan) in that order. Scale bars are 2 μm .

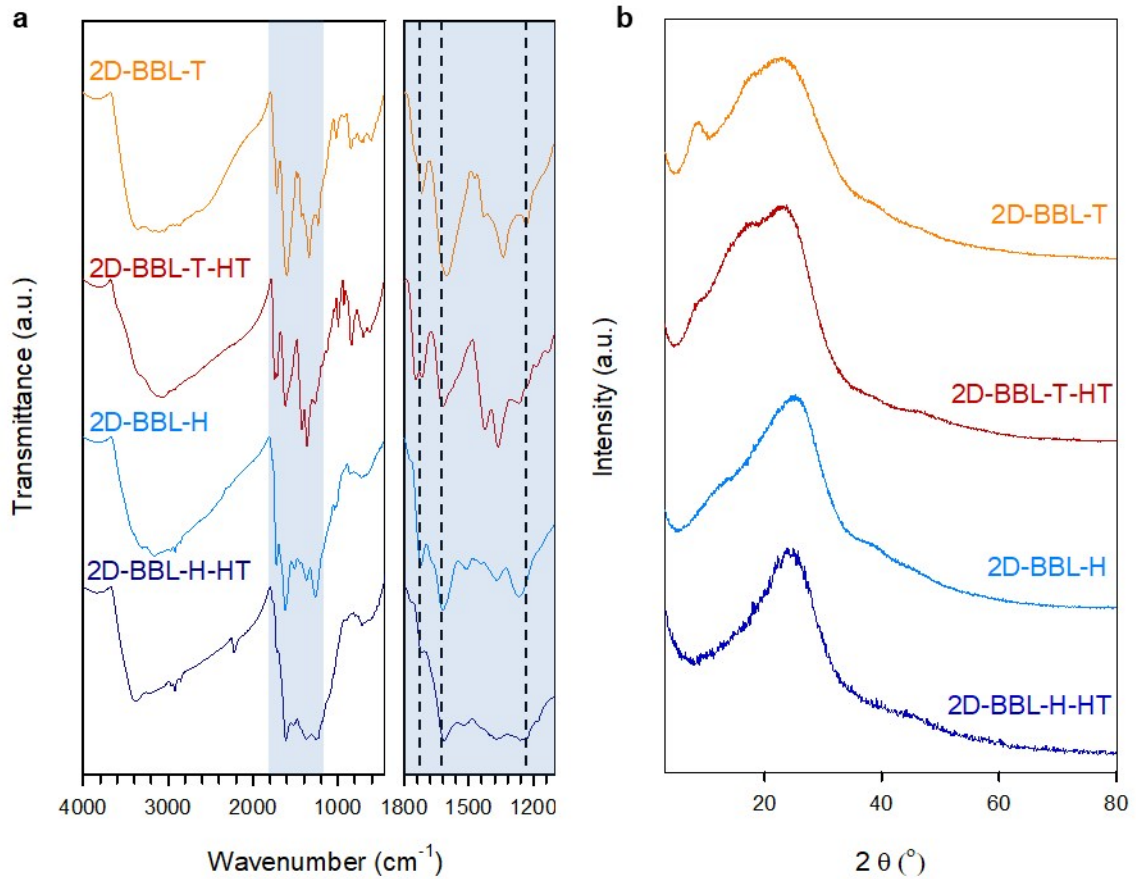


Fig. S6. FT-IR full spectra and **(b)** PXRD patterns for 2D-BBL-T, 2D-BBL-T-HT, 2D-BBL-H and 2D-BBL-H-HT.

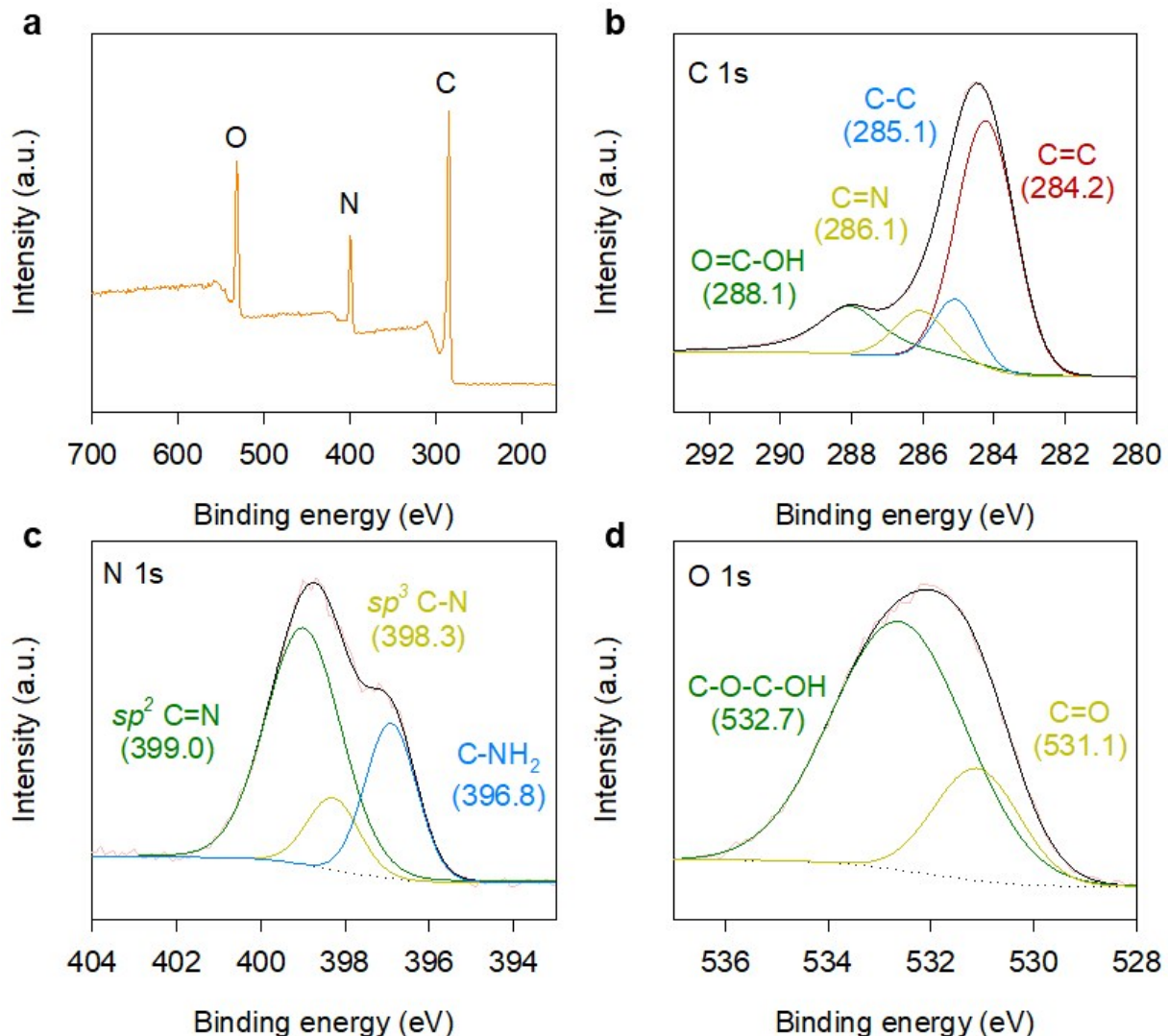


Fig. S7. XPS survey spectra of 2D-BBL-T: (a) Full spectra, (b) C 1s, (c) N 1s and (d) O 1s.

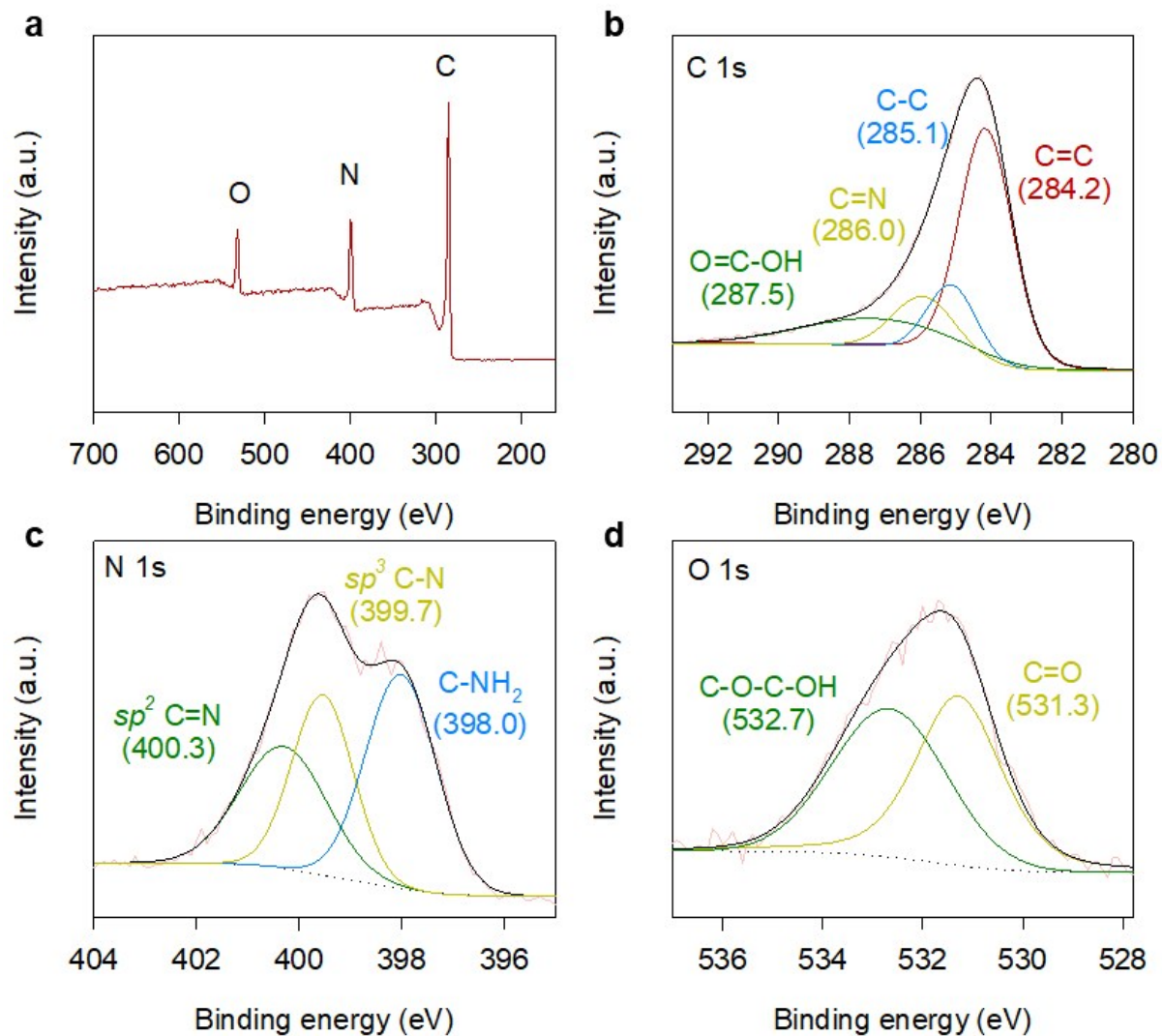


Fig. S8. XPS survey spectra of 2D-BBL-T-HT: **(a)** Full spectra, **(b)** C 1s, **(c)** N 1s and **(d)** O 1s.

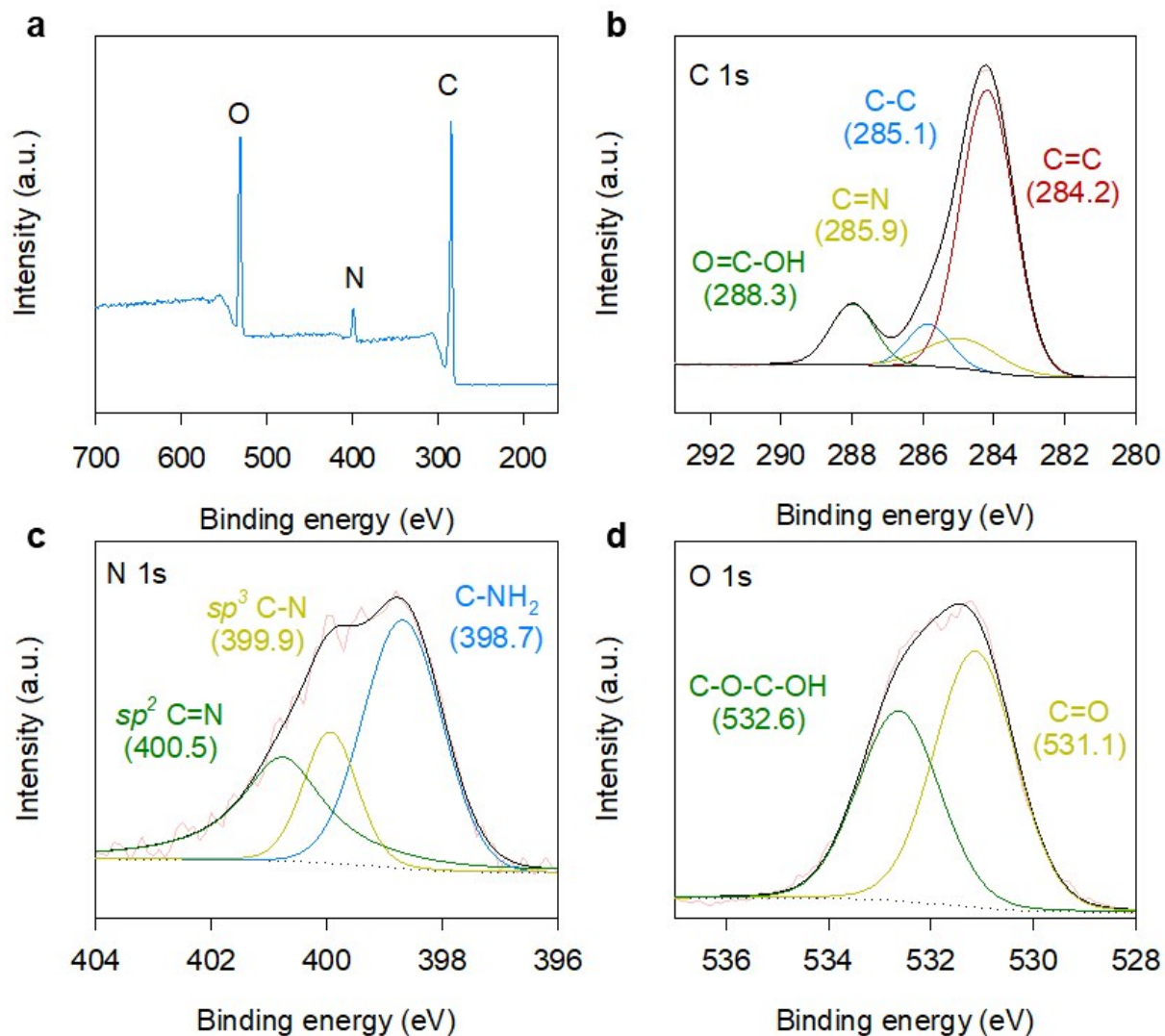


Fig. S9. XPS survey spectra of 2D-BBL-H: **(a)** Full spectra, **(b)** C 1s, **(c)** N 1s and **(d)** O 1s.

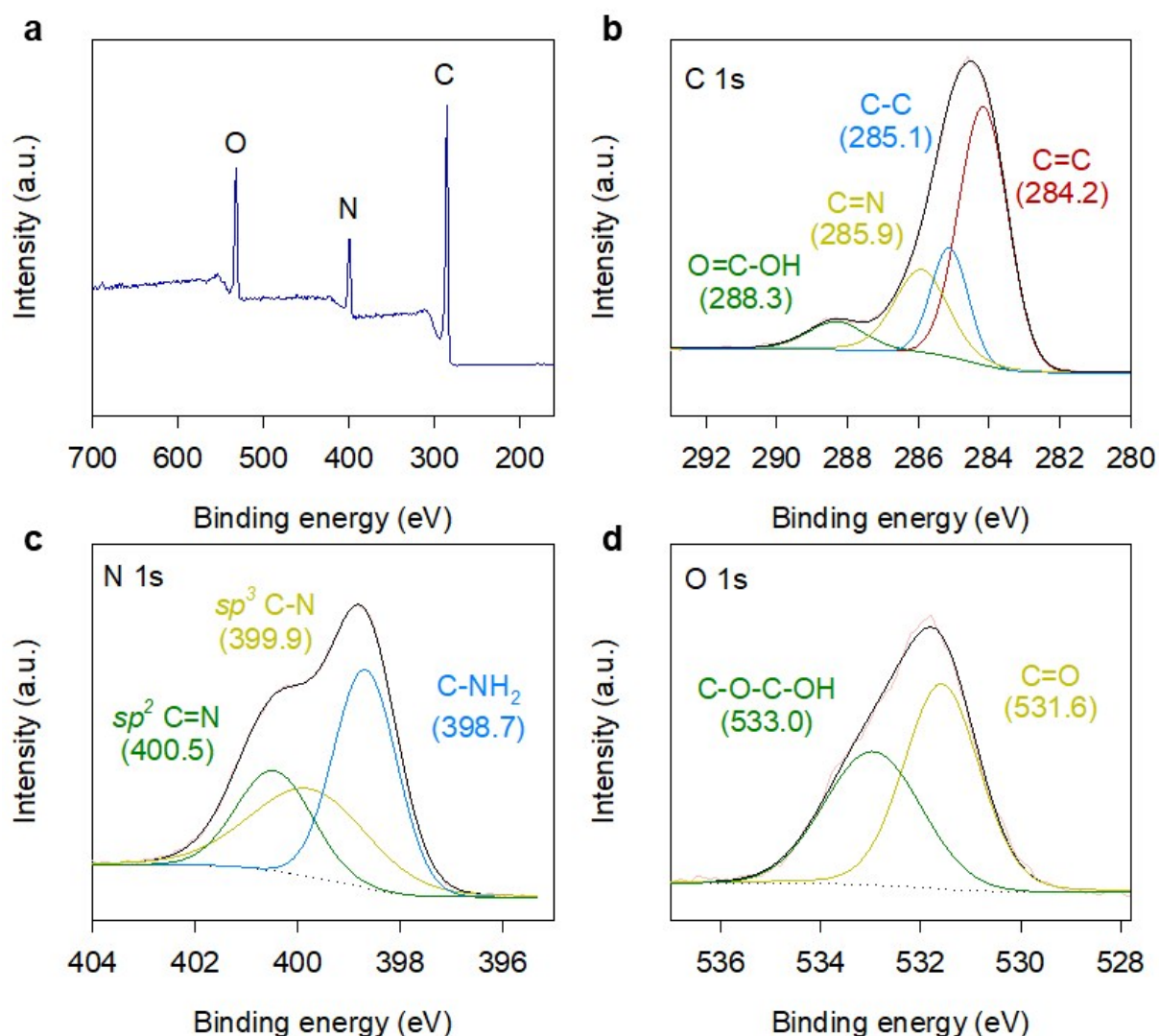


Fig. S10. XPS survey spectra of 2D-BBL-H-HT: (a) Full spectra, (b) C 1s, (c) N 1s and (d) O 1s.

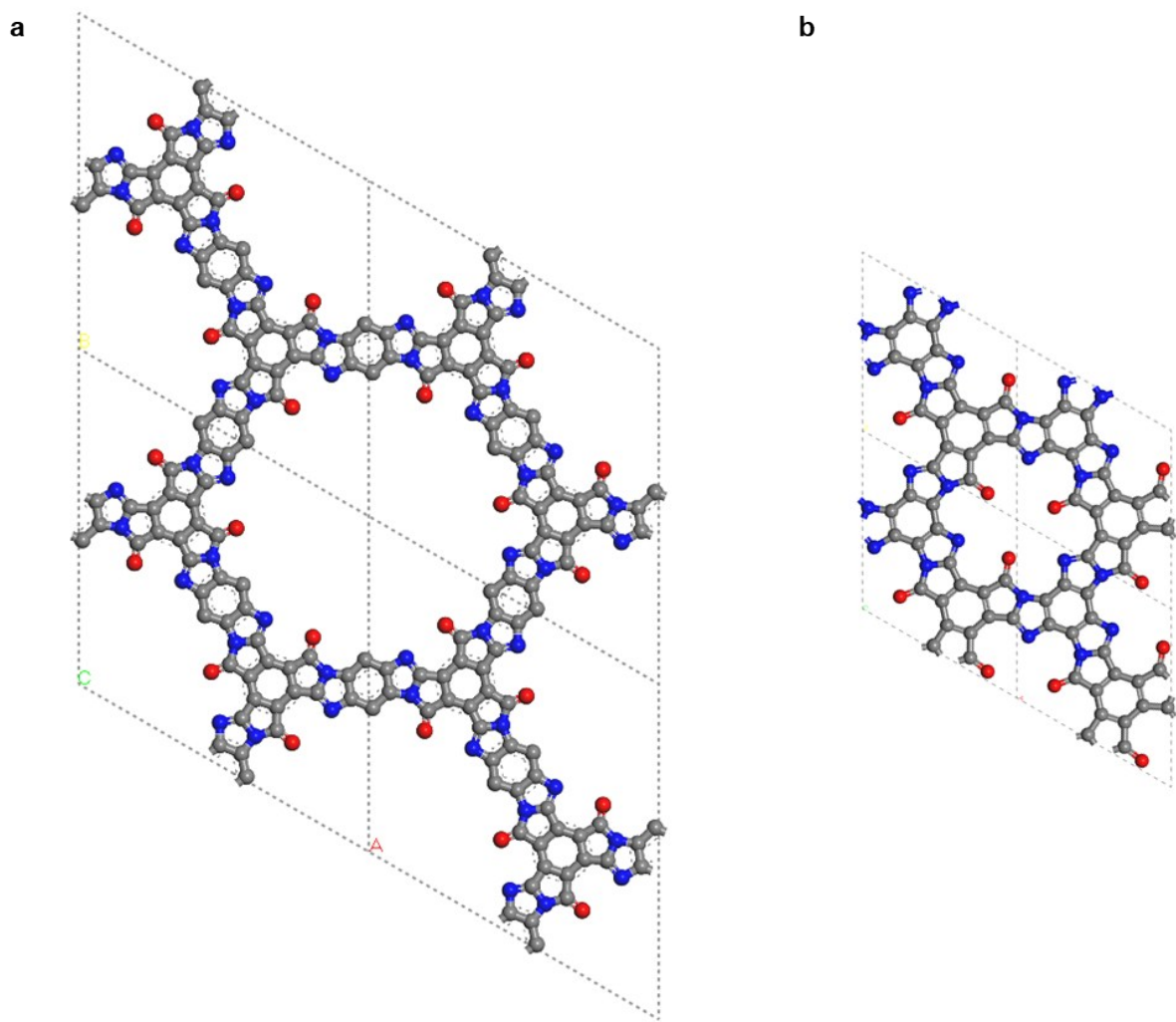


Fig. S11. Simulated unit cell structures: (a) 2D-BBL-T-HT and (b) 2D-BBL-H-HT (C, grey; N, blue; O, red).

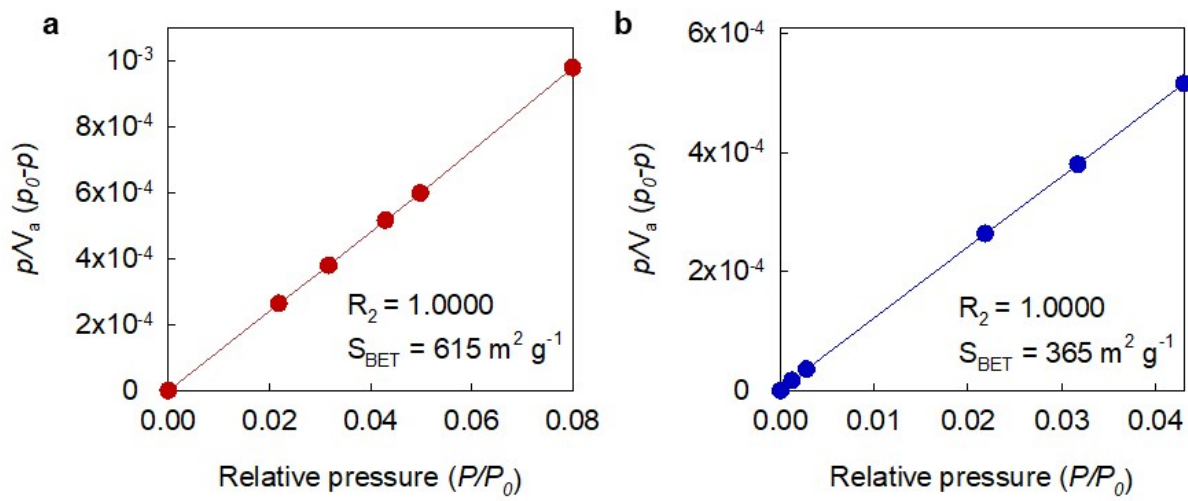


Fig. S12. BET plot of (a) 2D-BBL-T-HT and (b) 2D-BBL-H-HT at 77 K using nitrogen as adsorbate.

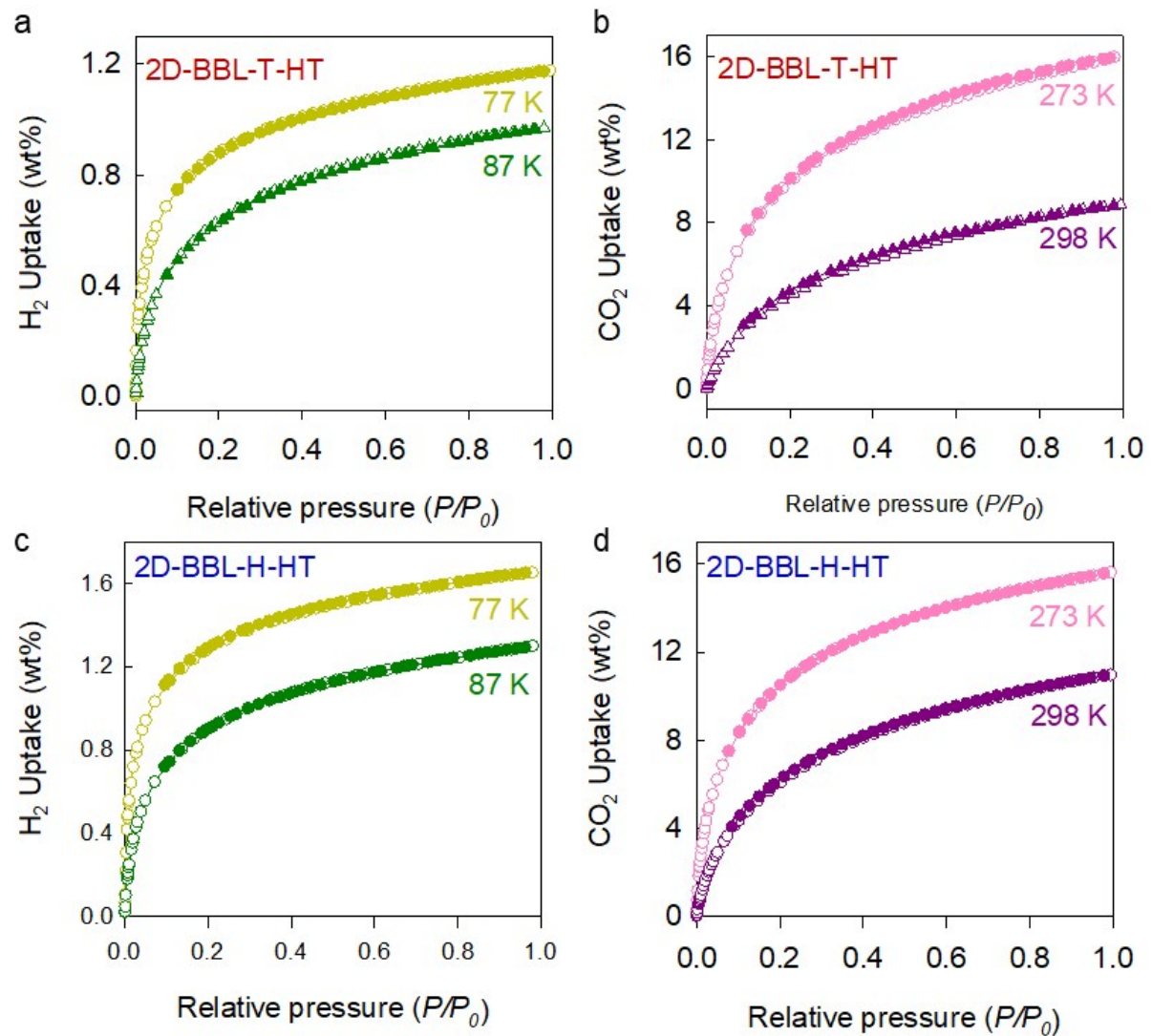


Fig. S13. Permanent porosities of 2D-BBL-T-HT: (a) H₂ adsorption-desorption isotherms at 77 K and 87 K, (b) CO₂ adsorption-desorption isotherms at 273 K and 298 K. Permanent porosities of 2D-BBL-H-HT: (c) H₂ adsorption-desorption isotherms at 77 K and 87 K, (d) CO₂ adsorption-desorption isotherms at 273 K and 298 K.

Table S1 | Elemental compositions of 2D-BBL-T and 2D-BBL-T-HT from various analytical techniques

	Element	C	N	O	H	C/N ratio
2D-BBL-T	Theoretical (wt.%)	65.13	21.70	12.39	0.78	3.00
	XPS (wt. %) ^a	66.18	14.36	19.46	-	4.60
	EA (wt. %)	49.05	16.62	30.52	3.74	2.95
	SEM EDS (wt.%) ^b	61.93	14.50	23.57	-	4.27
2D-BBL-T-HT	Theoretical (wt.%)	65.13	21.70	12.39	0.78	3.00
	XPS (wt. %)	71.57	18.77	9.66	-	3.81
	EA (wt. %)	60.00	20.75	12.25	3.20	2.89
	SEM EDS (wt.%)	63.96	15.13	20.91	-	4.23

a, b: more sensitive to surface chemical composition.

Table S2 | Elemental compositions of 2D-BBL-H and 2D-BBL-H-HT from various analytical techniques

	Element	C	N	O	H	C/N ratio
2D-BBL-H	Theoretical (wt.%)	65.13	21.70	12.39	0.78	3.00
	XPS (wt. %) ^a	66.94	6.52	26.54	-	10.27
	EA (wt. %)	49.47	16.66	27.30	3.25	2.97
	SEM EDS(wt.%) ^b	54.48	14.02	31.50	-	3.88
2D-BBL-H-HT	Theoretical (wt.%)	65.13	21.70	12.39	0.78	3.00
	XPS (wt. %)	66.69	14.91	18.40	-	4.47
	EA (wt. %)	55.37	23.01	18.48	2.52	2.40
	SEM EDS(wt.%)	58.61	19.11	22.28	-	3.07

a, b: more sensitive to surface chemical composition.

Table S3 | Comparison of the heat of adsorption of CO₂ by different materials

Class	Adsorbent Material	Pressure (atm)	Temperature (°C)	Qst (kJ mol ⁻¹)	References
Porous polymers	2D-BBL-T-HT	1	25	37.80	This work
	2D-BBL-H-HT	1	25	44.43	
	HCP	1.13	25	23.5	S ¹
	AAM-Silica	45	0.1	37	S ²
	3D-CON	1	25	31.87	S ³
	GO frameworks	4.0	25	35	S ⁴
Carbon-based Materials	p-CTF-1	1	25	30.7	S ⁵
	Leather derived AC	1	35	8	S ⁶
	AC	1	25	3	S ⁷
	AC (ZL-30)	1	25	10.5	S ⁸
MOFs	Ni(dobdc)	1	25	31.2	S ⁹
	Pd(2-pymo) ₂	0.5	25	26	S ¹⁰
	Mg-MOF-74	1	25	47	S ¹¹
	B100-1000	1	25	33.9	S ¹²
	MOF1	1	25	35.4	S ¹³
	Bio-MOF-1	1	15	31.2	S ¹⁴
Zeolites	SAPO-34	0.1	25	39.4	S ¹⁵
	Zeolite T	0.1	25	33.6	S ¹⁵
	Commercial Zeolite	1	25	30	S ⁷

References

- S1. C. F. Martín, E. Stöckel, R. Clowes, D. J. Adams, A. I. Cooper, J. J. Pis, F. Rubiera and C. Pevida, *J. Mater. Chem.*, 2011, **21**, 5475-5483.
2. Y. Zhao, Y. Shen, L. Bai and S. Ni, *Appl. Surf. Sci.*, 2012, **261**, 708-716.
3. J. Mahmood, S.-J. Kim, H.-J. Noh, S.-M. Jung, I. Ahmad, F. Li, J.-M. Seo and J.-B. Baek, *Angew. Chem. Int. Ed.*, 2018, **57**, 3415-3420.
4. S. Gadipelli and Z. X. Guo, *Prog. Mater. Sci.*, 2015, **69**, 1-60.

5. Y. Soo-Young, M. Javeed, N. Hyuk-Jun, S. Jeong-Min, J. Sun-Min, S. Sun-Hee, I. Yoon-Kwang, J. In-Yup and B. Jong-Beom, *Angew. Chem. Int. Ed.*, 2018, **57**, 8438-8442.
6. J. Bermúdez, P. Dominguez, A. Arenillas, J. Cot, J. Weber and R. Luque, *Materials*, 2013, **6**, 4641-4653.
7. M. Radosz, X. Hu, K. Krutkramelis and Y. Shen, *Ind. Eng. Chem. Res.*, 2008, **47**, 3783-3794.
8. B. Guo, L. Chang and K. Xie, *J. Nat. Gas Chem.*, 2006, **15**, 223-229.
9. W. L. Queen, M. R. Hudson, E. D. Bloch, J. A. Mason, M. I. Gonzalez, J. S. Lee, D. Gygi, J. D. Howe, K. Lee, T. A. Darwish, M. James, V. K. Peterson, S. J. Teat, B. Smit, J. B. Neaton, J. R. Long and C. M. Brown, *Chem. Sci.*, 2014, **5**, 4569-4581.
10. A. Ö. Yazaydin, R. Q. Snurr, T.-H. Park, K. Koh, J. Liu, M. D. LeVan, A. I. Benin, P. Jakubczak, M. Lanuza, D. B. Galloway, J. J. Low and R. R. Willis, *J. Am. Chem. Soc.*, 2009, **131**, 18198-18199.
11. S. R. Caskey, A. G. Wong-Foy and A. J. Matzger, *J. Am. Chem. Soc.*, 2008, **130**, 10870-10871.
12. H. R. Kim, T.-U. Yoon, S.-I. Kim, J. An, Y.-S. Bae and C. Y. Lee, *RSC Adv.*, 2017, **7**, 1266-1270.
13. S. S. Dhankhar and C. M. Nagaraja, *New J. Chem.*, 2018, DOI: 10.1039/C8NJ04947E.
14. J. An and N. L. Rosi, *J. Am. Chem. Soc.*, 2010, **132**, 5578-5579.
15. M. Salmasi, S. Fatemi, M. Doroudian Rad and F. Jadidi, *Int. J. Environ. Sci. Technol.*, 2013, **10**, 1067-1074.